The high $E°$ for the Ru(V/III) couple renders $[Ru^{V}(N_4O)O]^{2+}$ capable of oxidizing Cl^- to Cl_2 in aqueous solution. Similar results were obtained by Meyer and co-workers based on the $[(bpy)_2(O)Ru^{V}]_2O^{4+}$ dimeric species.[40] This suggests that oxidation of Cl^- to Cl_2 depends only on the redox potential of the oxidant concerned, irrespective of its dimeric or monomeric nature.

The observation that $[Ru^{V}(N_4O)O]^{2+}$ is capable of oxidizing the unactivated C-H bond in cyclohexane leads us to believe that high-valent ruthenium-oxo complexes, if suitably designed, have potential application in selective oxidation of alkanes. We believe that the ability of $[Ru^{V}(N_4O)O]^{2+}$ in cyclohexane oxidation probably lies in its high redox potential since other complexes such as *trans*-$[Ru^{VI}(TMC)O_2]^{2+}$[3a] and $[Ru^{IV}(trpy)(bpy)O]^{2+}$[41] having lower reduction potentials are found to be relatively unreactive in cyclohexane oxidation.

In a previous study, it has been found that *trans*-dioxoruthenium(V) of amines rapidly disproportionates in solution[4b] and that Ru(IV)=O complexes such as *trans*-$[Ru^{IV}(TMC)O(CH_3CN)]^{2+}$[3d] and $[Ru^{IV}(trpy)(bpy)O]^{2+}$[41] remain stable in acidic solutions. In this work, the $[Ru^{V}(N_4O)O]^{2+}$ ion remains stable in acidic solution, whereas the $[Ru^{IV}(N_4O)O]^{+}$ ion disproportionates. It thus appears that the stability of Ru=O complexes toward disproportionation may not have any correlation with the oxidation state and hence electronic configuration of the central ruthenium ion. The nonlabile coordinated ligands, which will affect the redox potentials of the Ru=O complexes and the pK_a values of the "Ru=O" moiety may contribute significantly to the stability of Ru=O complex in a given oxidation state.

Acknowledgment. Financial support from the University of Hong Kong and the Croucher Foundation (C.M.C. and V.W.W.Y.) are gratefully acknowledged. We thank Clare Ho for repeating some of the stoichiometric oxidations in acetonitrile. V.W.W.Y. acknowledges the receipt of scholarships from Li Po Chun and Croucher Foundation.

Supplementary Material Available: Tables of hydrogen atomic coordinates and thermal parameters and anisotropic thermal parameters, rotating disk voltammogram of $[Ru^{III}(N_4O)OH_2](ClO_4)_2$ in pH 4 acetate buffer, (Figure S1), spectrophotometric redox titration of $[Ru^{V}(N_4O)(O)](ClO_4)_2$, (Figure S2), and IR spectrum of $[Ru^{V}(N_4O)(O)](ClO_4)_2$ (Figure S3) (5 pages); table of observed and calculated structure factors (21 pages). Ordering information is given on any current masthead page.

(40) (a) Ellis, C. D.; Gilbert, J. A.; Murphy, W. R., Jr.; Meyer, T. J. *J. Am. Chem. Soc.* **1983**, *105*, 4842. (b) Vining, W. J.; Meyer, T. J. *Inorg. Chem.* **1986**, *25*, 2023.

(41) Moyer, B. A.; Thompson, M. S.; Meyer, T. J. *J. Am. Chem. Soc.* **1980**, *102*, 2310.

Solid-Phase Peptide Synthesis of the α and β Domains of Human Liver Metallothionein 2 and the Metallothionein of *Neurospora crassa*

F. Jon Kull,[†] Michael F. Reed,[†] Timothy E. Elgren,[†] Thomas L. Ciardelli,[‡] and Dean E. Wilcox*,[†]

Contribution from the Department of Chemistry, Dartmouth College, Hanover, New Hampshire 03755, and Department of Pharmacology and Toxicology, Dartmouth Medical School, Hanover, New Hampshire 03756. *Received February 21, 1989*

Abstract: The Cys-rich peptides corresponding to the α and β domains of human liver metallothionein 2 (MT-2) and the MT from *Neurospora crassa* (NcMT) have been prepared for the first time by solid-phase peptide synthesis and purified by HPLC. These synthetic peptides bind Cd(II), Ag(I), and Cu(I) in identical stoichiometries with the proteolytically derived domains from rat and rabbit liver MT and the natural NcMT. Absorption and CD features observed upon Cd(II) and Cu(I) binding to the synthetic peptides are qualitatively similar to those reported for the natural domains and NcMT. ^{113}Cd NMR of the synthetic Cd_4 α domain indicates that three of the metal ions are in environments identical with those in the whole protein and in the proteolytically derived α domain; the chemical shift of the fourth Cd(II), which is located near the junction with the β domain, indicates this metal ion is in a somewhat different environment than in the native protein. Thus, we have shown that it is possible to use solid-phase peptide synthesis to prepare MT. This demonstrates the successful use of solid-phase methods for peptides with high Cys content and now provides a methodology for the facile sequence modification of MT.

Metallothioneins (MT)[1] are a class of small (~61 amino acids), ubiquitous, cysteine-rich (~30%) proteins that typically bind 7 (Cd(II), Zn(II)) or ~12 (Cu(I), Ag(I)) metal ions through metal-thiol ligation. They have been shown to bind essential (Cu(I), Zn(II)) as well as toxic (Cd(II), Hg(II)) metal ions in vivo, and although their biological role is not clear, it is likely they are involved in metal ion metabolism. The 25-residue MT from *Neurospora crassa* (NcMT) shows[2] Cys homology with the N-terminal (β) domain of MT from higher organisms and appears to play a role in Cu metabolism in the fungus.

Initial ^{113}Cd NMR studies[3] of Cd_7MT indicated that this metal ion was bound in isolated three- and four-metal clusters with Cys ligation. Subsequently, enzymatic cleavage methods were developed to isolate[4] the 31-61-residue α domain that binds the four-Cd(II) cluster and later separate[5] the 1-31-residue β domain that binds the three-Cd(II) cluster. Proteolytic preparation of the two domains is possible on the basis of differential metal ion binding by the two peptide segments; Cd(II) binds more strongly as a four-ion cluster in the α domain and stabilizes it toward

* To whom correspondence should be addressed.
[†] Dartmouth College.
[‡] Dartmouth Medical School.

(1) (a) Kagi, J. H. R., Nordberg, M., Eds. *Metallothionein*; Birkhauser Verlag: Basel, 1979. (b) Kagi, J. H. R., Kojima, Y., Eds. *Metallothionein II*; Birkhauser Verlag: Basel, 1987.
(2) Lerch, K. *Nature* **1980**, *284*, 368-370.
(3) Otvos, J. D.; Armitage, I. M. *Proc. Natl. Acad. Sci. U.S.A.* **1980**, *77*, 7094-7098.
(4) Winge, D. R.; Miklossy, K.-A. *J. Biol. Chem.* **1982**, *257*, 3471-3476.
(5) Nielson, K. B.; Winge, D. R. *J. Biol. Chem.* **1984**, *259*, 4941-4946.

0002-7863/90/1512-2291$02.50/0

proteolytic degredation, while Cu(I) preferentially binds and stabilizes the β domain. ^{113}Cd NMR of the Cd_4 α domain has shown[6] that the environment of the Cd(II) ions is not significantly perturbed in the proteolytically isolated domain. The recent X-ray crystallographic structure of Cd_5Zn_2MT-2 (MT-2 = metallothionein 2) from rat liver has confirmed[7] and elaborated this structural picture consisting of two peptide domains each containing a metal ion cluster; NMR studies[8] support this basic structure but have identified discrepancies between the metal ion coordination in crystalline and solution samples.

The properties of the individual MT domains have been characterized recently through studies of the metal ion stoichiometry of each domain,[9] Co(II) binding by the α domain,[10] the structure of the Cu_6 β domain (X-ray absorption and EXAFS measurements),[11] and metal ion binding to each domain (absorption, CD, and MCD data).[12] Future studies of the individual domains will be important for quantifying metal ion exchange between the domains, providing a simpler model to elucidate the biophysics of metal–Cys interaction, evaluating the possibility of interdomain interaction (cooperativity) in metal ion binding, and possibly resolving structural discrepancies between NMR and crystallography.

The ~30 amino acid MT domains are small enough to be synthetically prepared; however, the large number of cysteine residues might be expected to result in oxidative complications during synthesis and purification. Nevertheless, bench-top solution chemistry employing azide coupling of small peptide fragments has been used to synthesize the α[13] and β[14] domains of human liver MT-2, although the metal-binding properties of these peptides were not well characterized. However, classical solution peptide synthesis is a tedious technique requiring isolation and purification of the synthetic intermediates. Automated solid-phase peptide synthesis presents a more rapid and efficient alternative for protein synthesis *and primary structure modification.* Further, the small size and unique amino acid content of MT may result in it being less amenable to residue modification by the molecular genetic approach of site-selective mutagenesis and overproduction in a host. While there has been one brief report[15] of an attempt to prepare NcMT by solid-phase techniques, it is uncertain whether the synthesis was successful due to difficulties in purification; the product was not characterized.

As part of our studies of the coordination chemistry of metallothionein we have undertaken its synthetic preparation. In this our initial effort, we have shown that in spite of the high Cys content the ~30 residue domains of mammalian MT and the 25 residue NcMT can be synthesized by solid-phase methods and purified by HPLC in reasonable yield and that these synthetic Cys-rich peptides have similar metal ion binding properties as the natural peptides.

Experimental Section

Peptide Synthesis, Purification, and Analysis. Automated synthesis of the 25- to 31-residue peptides was accomplished with Boc-protected L amino acids (Biosearch) and a Biosearch 9500 automated solid-phase peptide synthesizer. Protection of amino acid third functionalities included *O*-cyclohexylaspartic acid, *S*-(4-methylbenzyl)cysteine, *O*-benzylglutamic acid, *N*-(*o*-chlorobenzyloxycarbonyl)lysine, *O*-benzylserine, and *O*-benzylthreonine. As a solid support, 1 g of 4-methylbenzhydrylamine resin (Biosearch) with 0.31 mmol/g substitution was employed for the β-domain synthesis and 1 g of Boc-X-PAM resin (Du Pont) with 0.40 mmol/g substitution (X = Ala) and 0.30 mmol/g substitution (X = Lys) was used for the α domain and NcMT syntheses, respectively. Amino acids (0.4 M in dimethylformamide (DMF)) were added in 6.67-fold excess; Asn and Gln coupling was facilitated with 1-hydroxybenzotriazole to prevent dehydration side reactions. Each consecutive residue was deprotected with a solution consisting of 45% trifluoroacetic acid (TFA), 2.5% anisole, 2% 1,2-ethanedithiol, and 50.5% dichloromethane (DCM); neutralization of the resulting TFA salt was accomplished with redistilled diisopropylethylamine (10% in DCM); coupling was mediated with 0.4 M 1,3-diisopropylcarbodiimide in DCM; and capping of the unreacted amino groups was effected with 1-acetylimidazole (0.3 M in DMF). Reagents for these solutions were obtained from Aldrich. The protected peptide resin was washed two or three times each with DCM and methanol and dried in a vacuum desiccator for 48 h. Half of the β-domain synthesis product was subsequently capped by acetylation of the N-terminal Met with 0.4 M 1-acetylimidazole in DMF.

The peptide products were cleaved and deprotected by anhydrous HF treatment with a Biosearch HF apparatus. In the initial synthesis of the unacetylated β domain, 50 mg of L-Met and 1.2 mL of anisole were added as a carbocation scavenger with 1.20 g of the resin/product. Product yields were improved for the α domain and NcMT by use of 0.625 g each of *p*-thiocresol and *p*-cresol with 1.25 g of the resin/product.[16] The scavenger and resin/product were placed in the Teflon reaction vessel, which was then exhaustively purged with nitrogen and cooled in a dry ice/propanol bath. HF was then condensed into the vessel (total volume 12 mL) and allowed to stir vigorously for 1 h at 0 °C, after which the HF was removed by vacuum. A 20-mL portion of ethyl acetate was then added, and the product was filtered on a Büchner funnel with three ethyl acetate washes. The crude product was extracted from the resin with deoxygenated cold 1 N acetic acid (5 mM EDTA) and lyophilized.

A low-high HF procedure[17] was used to cleave and deprotect the acetylated β-domain peptide. A 1.05-g sample of the peptide resin was stirred vigorously for 2 h at 0 °C in the Teflon reaction vessel with 10 mL of a cleavage mixture consisting of HF, dimethyl sulfide (DMS), and anisole in a 25/65/10% ratio (the DMS had been filtered on basic alumina) followed by the anhydrous HF cleavage procedure described above. This procedure appeared to improve the product yield somewhat.

Analytical and preparative HPLC was performed with a Waters 840 HPLC system equipped with a Waters 712 WISP autosampler. A W-POREX 5 C_4 column (4.6 mm × 7.5 cm, Phenomenex) was used for analytical HPLC and a DYNAMAX MACRO C_8 column for preparative HPLC. Protein samples were dissolved in deoxygenated 6 M guanidine hydrochloride or aqueous TFA solutions. Gradient elution was employed with mobile phases consisting of water and acetonitrile containing 0.1% TFA; the eluate was monitored at 215 nm. All solvents used in the synthesis and purification were HPLC grade (VWR, OmniSolv).

Amino acid composition of the peptides was determined with a Waters PICO·TAG system by acid hydrolysis of the peptide for 24, 48, or 72 h, amino acid derivatization with phenyl isothiocyanate (PITC), and relative quantification of the amino acids by analytical HPLC. Peak areas of individual derivatized amino acids of the sample and of a standard mixture (250 pmol each) of (phenylthio)carbamyl amino acids were integrated and used to calculate the amino acid content of the peptide.

Amino acid sequence analysis of the synthetic NcMT peptide was performed by the Biotechnology Institute Sequence Facility at Cornell University. The *S*-carboxyamido-methylated derivative was prepared as previously described[18] and shown to be homogeneous by analytical HPLC prior to sequence analysis.

Metal Ion Binding. All solutions used in metal ion binding studies were prepared with deionized water passed through a Chelex 100 (Bio-Rad) column and thoroughly deoxygenated before use. Peptide solutions were prepared by weighing 0.5–2 mg (±0.02 mg) of the lyophilized material on a Mettler M5 ultramicro balance. Lyophilized MT may contain[19] as much as 25% water by weight; the concentrations of peptide

(6) Boulanger, Y.; Armitage, I. M.; Miklossy, K.-A.; Winge, D. R. *J. Biol. Chem.* **1982**, *257*, 13717–13719.
(7) Furey, W. F.; Robbins, A. H.; Clancy, L. L.; Winge, D. R.; Wang, B. C.; Stout, C. D. *Science* **1986**, *231*, 704–710.
(8) Wagner, G.; Neuhaus, D.; Worgotter, E.; Vasak, M.; Kagi, J. H. R.; Wuthrich, K. *Eur. J. Biochem.* **1986**, *157*, 275–289.
(9) Nielson, K. B.; Winge, D. R. *J. Biol. Chem.* **1985**, *260*, 8698–8701.
(10) Good, M.; Vasak, M. *Biochemistry* **1986**, *25*, 3328–3334.
(11) George, G. N.; Winge, D. R.; Stout, C. D.; Cramer, S. P. *J. Inorg. Biochem.* **1986**, *27*, 213–220.
(12) (a) Zelazowski, A. J.; Szymanska, J. A.; Law, A. Y. C.; Stillman, M. J. *J. Biol. Chem.* **1984**, *259*, 12960–12963. (b) Stillman, M. J.; Cai, W.; Zelazowski, A. J. *J. Biol. Chem.* **1987**, *262*, 4538–4548.
(13) Okada, Y.; Ohta, N.; Yagyu, M.; Min, K.-S.; Onosaka, S.; Tanaka, K. *J. Protein Chem.* **1984**, *3*, 243–257.
(14) (a) Okada, Y.; Ohta, N.; Yagyu, M.; Min, K.-S.; Onosaka, S.; Tanaka, K. *FEBS Lett.* **1985**, *183*, 375–378. (b) Okada, Y.; Ohta, N.; Iguchi, S.; Tsuda, Y.; Sasaki, H.; Kitagawa, T.; Yagyu, M.; Min, K.-S.; Onosaka, S.; Tanaka, K. *Chem. Pharm. Bull.* **1986**, *34*, 986–998.
(15) Leib, T. K.; Su, T.-M.; Holms, D. S. DOE Report DOE/ER/13278-2, 1986.
(16) Heath, W. F.; Tam, J. P.; Merrifield, R. B. *Int. J. Peptide Protein Res.* **1986**, *28*, 498–507.
(17) Tam, J. P.; Heath, W. F.; Merrifield, R. B. *J. Am. Chem. Soc.* **1983**, *105*, 6442–6455.
(18) McCormick, C. C.; Fullmer, C. S.; Garvey, J. S. *Proc. Natl. Acad. Sci. U.S.A.* **1988**, *85*, 309–313.
(19) Liberatore, F. A.; Comeau, R.; Morelock, M. M. Personal communication.

Table I. Amino Acid Analysis Data for the Synthetic Peptides

amino acid	β domain		α domain[a]		*N. crassa* MT[a]	
	expected	obtained	expected	obtained	expected	obtained
Ala	3	3.28	4	4.40	1	1.05
Asx (Asp, Asn)	3 (2Asp) (1 Asn)	2.69	1 (Asp)	0.87	3 (2 Asn) (1 Asp)	2.77
Cys	9	8.89	11	11.56[b]	7	6.61[b]
Glx (Glu, Gln)	1 (Glu)	1.12	1 (Gln)	0.99		
Gly	2	2.19	2	2.28	6	6.41
Ile			1	0.83		
Lys	3	3.14	4	3.55	1	0.90
Met	1	1.14				
Pro	1	0.92	1	1.10		
Ser	4	2.80	5	4.5[c]	7	6.40[c]
Thr	2	2.00				
Val			1	1.56		

[a] Average of two sets of determinations, except for Cys and Ser. [b] Cysteic acid determination. [c] Extrapolation of 24-, 48-, and 72-h acid hydrolysis data back to $t = 0$.

solutions used in this study were not corrected for the water content of the lyophilized peptides. All glassware and plasticware were cleaned with nitric acid and a 10 mM EDTA solution and repeatedly rinsed with deionized water.

Atomic absorption spectroscopy (AAS) was used to monitor metal ion binding, based on the method of Nielson and Winge[9] with $CdCl_2 \cdot 2.5H_2O$ (Mallinckrodt analytical reagent), Ag(I) (Aldrich 1000 ppm AAS standard), and $Cu(CH_3CN)_2Cl$ (prepared by the method of Lontie et al.[20]). For example, one Ag(I) binding analysis was performed as follows: 0.572 mg of the peptide was dissolved in 4 mL of 50 mM acetic acid (pH 2.8); this solution was split into 400-μL samples to which were added 100-μL aqueous aliquots containing different Ag(I) concentrations; this was followed by 200 μL of a 0.4 M HEPES (Sigma) pH 7.5 solution to raise the pH; after 45 min, 800 μL of an aqueous Chelex 100 slurry (1 g/10 mL) was added; the resultant mixture was incubated for 30 min and then separated by centrifugation to remove unbound metal ions. The supernate protein solutions were diluted with 1% HNO_3 in deionized water for analysis of metal ion content on a Perkin-Elmer 503 atomic absorption spectrometer with HGA-2100 controller and graphite furnace or a Thermo Jarrel Ash atomic absorption spectrometer with graphite furnace and Fastac atomizer.

Spectrophotometric analysis of metal ion binding was performed on samples prepared as indicated above for AAS. UV absorption measurements were performed at room temperature in 1-cm quartz cuvettes on a Perkin-Elmer λ-9, Cary 14, or Hewlett-Packard 8451A spectrophotometer. CD spectra were obtained at room temperature on an Instruments SA Mark V circular dichrograph.

^{113}Cd NMR spectra of the Cd_4 α domain were obtained at 22 °C on a Varian XL-300 spectrometer operating at 55.5 MHz with continuous broad-band decoupling; chemical shifts are reported downfield from the ^{113}Cd resonance of 0.1 M $Cd(ClO_4)_2$. The acquisition parameters were 50-kHz spectral width, 0.336-s acquisition time, and 6-μs (10.8°) pulse angle; a line-broadening function of 5 Hz was applied prior to Fourier transformation. The sample was prepared by mixing a 0.4 M HEPES buffer solution (pH 4.0) containing $^{113}CdCl_2$ (CdO, 96% enriched with ^{113}Cd from Oak Ridge, in 0.1 M HCl) with 50 mM deoxygenated acetic acid (pH 3.0) containing the synthetic peptide in a 1 to 4 mol equiv ratio relative to Cd. The pH of this solution was adjusted to 7.0 with ultrapure NaOH followed by addition of 20 g of Chelex 100 resin; this solution sat overnight at 4 °C. The resin was then removed by filtration, the sample was diluted into a 50 mM Tris (pH 7.1) solution containing 0.5 M NaCl, and finally, the solution was concentrated to ~1.2 mL; 10% D_2O was added to provide a frequency lock.

Results

Synthesis. Three peptides corresponding to the β domain (residues 1–29) and the α domain (residues 31–61) of human liver metallothionein 2 and the entire 25-residue metallothionein from *N. crassa* were synthesized by solid-phase peptide methods using Boc-protected amino acids and purified by reversed-phase HPLC. The N-terminal Met of half of the synthetic β domain was acetylated as is found for the natural peptide. Due to the high Cys content (31%, 35%, and 28%, respectively) of these peptides, a variety of oxidized products can be obtained after cleavage from the resin and deprotection. For the β domain, the crude product could not be readily identified on the HPLC chromatogram. However, exhaustive reduction of the product (0.1 M Tris (pH 8.5)/6 M guanidine hydrochloride with either 100 mM dithiothreitol and 280 mM 2-mercaptoethanol or 250 mM dithiothreitol) led to the large enhancement of one analytical HPLC peak that was tentatively assigned as the fully reduced peptide; this material was purified by preparative HPLC. Aerobic oxidation (pH 8–9) of a small amount of the reduced material led to the disappearance of this analytical HPLC peak, suggesting formation of oxidized peptide species. For the α domain and NcMT, the presence of a thiolate, *p*-thiocresol, during cleavage and deprotection apparently suppressed peptide oxidation, and a major product peak was readily identified and purified by HPLC. In the purification of each peptide, optimum purity was sought and determined by quantitative analytical HPLC with a C_4 column to be 90–95% for the β domain, ~90% for the α domain, and 95% for NcMT. The unoptimized yields for these syntheses were 3% (30 mg) for the β domain, 4% (50 mg) for the α domain, and 6% (39 mg) for NcMT.

The amino acid composition of the synthetic peptides was determined by acid hydrolysis, PITC derivatization, and HPLC analysis. Since Cys and Ser can decompose under the acid hydrolysis conditions, in certain analyses Cys was oxidized to cysteic acid with performic acid (5 μL/mg of protein) prior to quantitation and Ser was quantified by extrapolating analytical data obtained after 24, 48, and 72 h of acid hydrolysis back to $t = 0$. Table I lists the expected composition of the synthetic peptides and the experimentally determined amino acid content. Excellent agreement is found for all residues. Additional confirmation of the correct identity of the synthetic NcMT protein was provided by amino acid sequence analysis carried out for 23 cycles, which showed the expected results, in particular correct placement of the Cys residues.

Characterization. To characterize the synthetic peptides, their metal ion binding properties have been determined for comparison with those reported for the proteolytically derived domains and the natural NcMT. In particular, UV absorption and CD spectral data for metal ion binding to the synthetic peptides have been obtained; features that appear in this spectral region upon addition of metal ions to apo- (metal-free) MT are assigned as thiolate-to-metal charge-transfer (CT) transitions.

The amount of metal ion bound to the apo peptides was monitored by AAS and showed (Figure 1) for Cd(II) an increase up to ~2.5 mol equiv for the β domain, 4 mol equiv for the α domain, and 2 mol equiv for NcMT. In addition, Ag(I) binding to the β domain did not increase beyond ~5 mol equiv, the amount of Cu(I) bound to the α domain did not increase significantly beyond 4 mol equiv and maximizes at ~6, and Cu(I) binding to NcMT appears to saturate at 6 mol equiv (additional Cu(I) may be binding at ≥10 mol equiv).

Upon Cd(II) addition to the β domain new absorption intensity is observed (Figure 2A) with a maximum at 247 nm in the dif-

(20) Lontie, R.; Blanton, V.; Albert, M.; Peeters, B. *Arch. Int. Physiol. Biochem.* **1973**, 150–152.

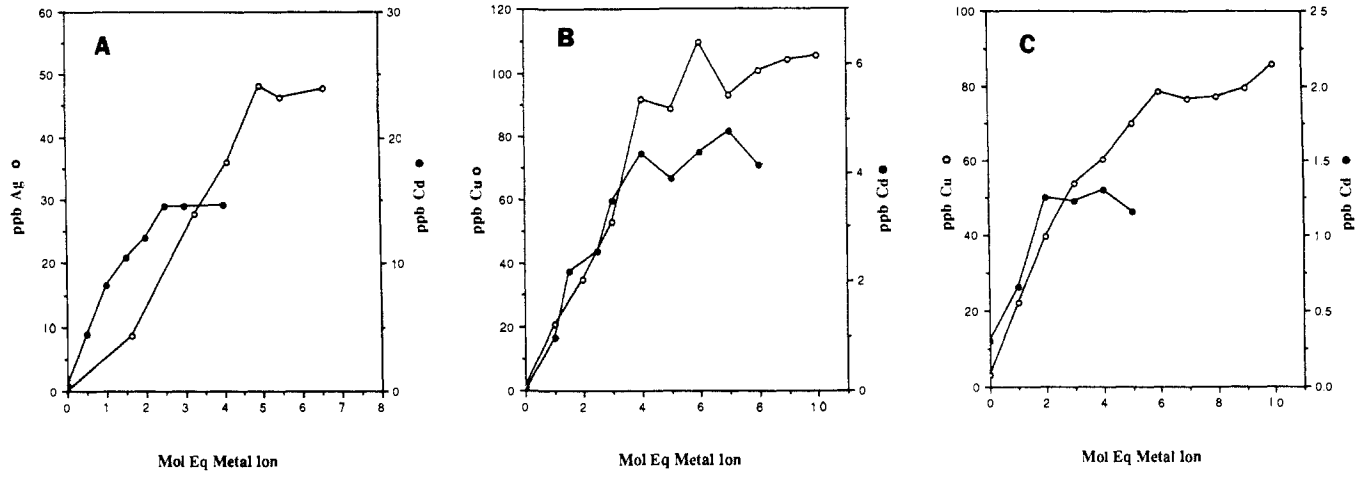

Figure 1. Atomic absorption analysis of the amount of metal ion bound to the synthetic (A) β domain (Cd(II), ●; Ag(I), ○), (B) α domain (Cd(II), ●; Cu(I), ○), and (C) NcMT (Cd(II), ●; Cu(I), ○) after addition of increasing mole equivalence of metal ion followed by treatment with Chelex 100. See text for experimental details.

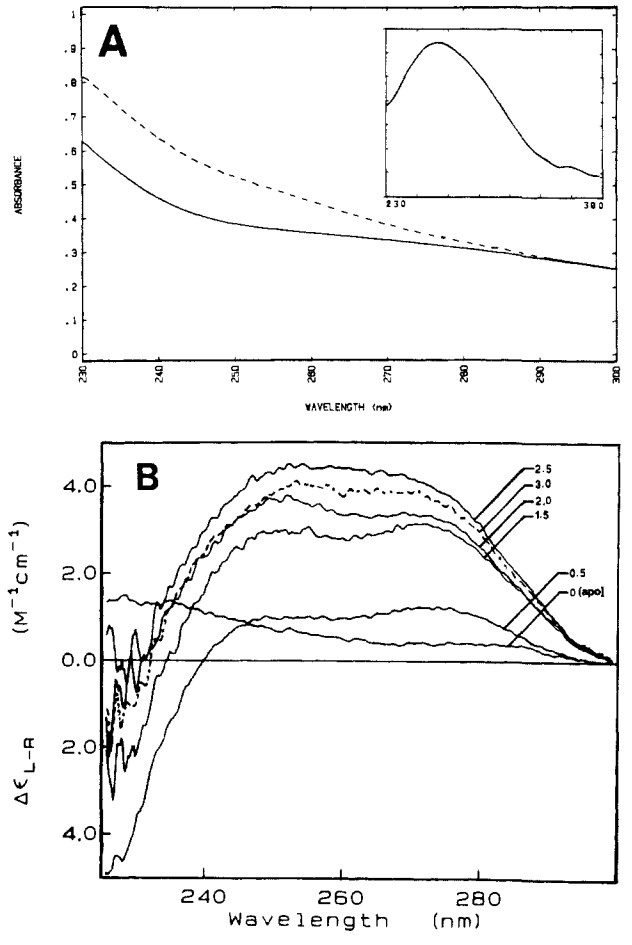

Figure 2. (A) UV absorption spectra of the synthetic β domain in the absence (—) and presence (---) of 3 mol equiv of Cd(II) (inset is the difference spectrum); (B) UV CD spectra of the synthetic β domain in the absence (apo) and presence of increasing mole equivalence of Cd(II) (the 3 mol equiv spectrum is indicated by the dashed line).

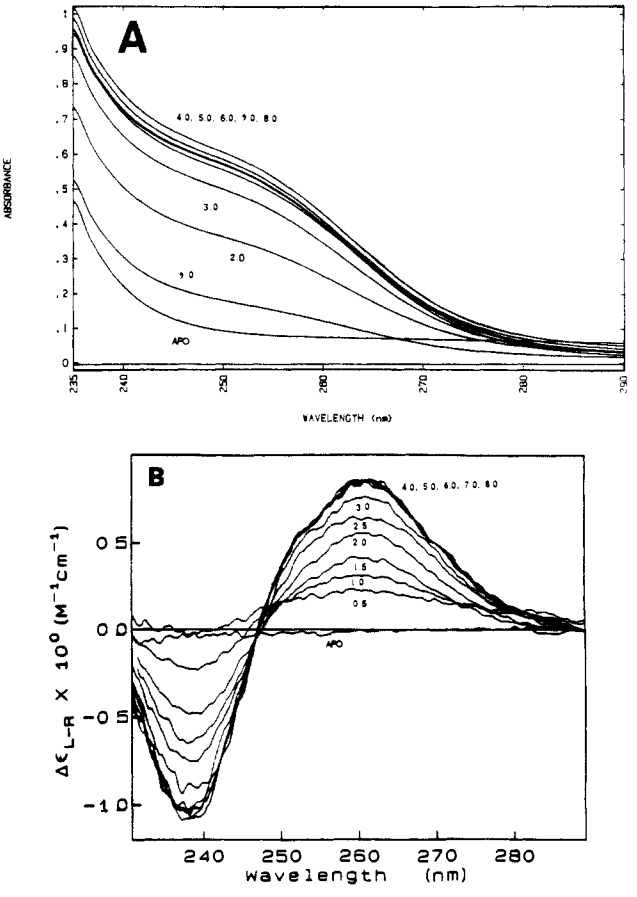

Figure 3. UV absorption (A) and CD (B) spectra of the synthetic α domain in the absence (apo) and presence of increasing mole equivalence of Cd(II).

ference spectrum (inset). The CD spectra of a Cd(II) titration of the unacetylated synthetic β domain in the 230–290-nm region (Figure 2B) show new positive features at 250 and 275 nm that increase in intensity up to 2.5 mol equiv of Cd(II), with a subsequent small decrease in intensity at 3 mol equiv; a similar decrease in the 247-nm absorption intensity is observed for >2.5 mol equiv of Cd(II). CD spectra of a Cd(II) titration of the acetylated domain (data not shown) are similar to those of the unacetylated peptide. Ag(I) binding to the synthetic β domain also leads to new absorption intensity, with a maximum at 232 nm and a shoulder at ~250 nm in the difference spectrum (data not shown).

Cd(II) binding to the synthetic α domain shows (Figure 3A) the appearance of an absorption shoulder at 250 nm, which reaches maximum intensity at 4 mol equiv of Cd(II). CD data in the same spectral region (Figure 3B) show a positive feature at 261 nm and a negative feature at 238 nm, each of which maximize in intensity at 4 mol equiv. To further characterize Cd(II) binding to this synthetic domain, we have obtained ^{113}Cd NMR data of the Cd_4 α domain. As shown in Figure 4, four resonances with approximately equal integrated intensity are found at 669, 630, 627, and 605 ppm downfield relative to $Cd(ClO_4)_2$; weak features are also

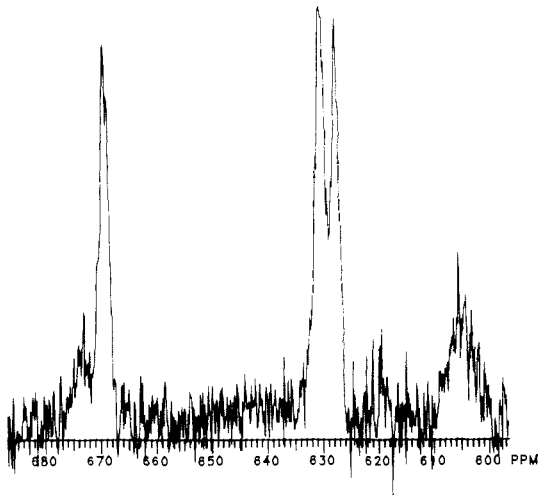

Figure 4. Proton-decoupled ^{113}Cd NMR spectrum of the $^{113}Cd_4$ α domain prepared from the synthetic peptide (~6.9 mM) in 50 mM Tris (pH 7.1) with 0.5 M NaCl. Spectrum was taken at 22 °C with 410 000 transients.

observed at 673 and 619 ppm. Cu(I) binding to the synthetic α domain results in a new absorption shoulder at 265 nm (Figure 5A) and a new positive CD band at 262 nm (Figure 5B). Each feature maximizes in intensity upon addition of 4 mol equiv of Cu(I); between 4 and 6 mol equiv the absorption intensity is observed to decrease and the positive CD intensity to be nearly eliminated. At >6 mol equiv of Cu(I) major changes appear in the absorption and CD spectra (data not shown), with increased absorption intensity and strong negative CD intensity that extends into the visible.

Cd(II) binding to the synthetic NcMT leads to a new absorption shoulder at ~250 nm (Figure 6A) and CD band at 245 nm (Figure 6B). The intensity of these electronic features increases only up to 2 mol equiv, paralleling the atomic absorption data, which indicates only 2 Cd(II) ions bind tightly to the synthetic NcMT. Cu(I) binding to this synthetic peptide has also been monitored spectroscopically with the absorption spectrum (Figure 7A) showing a shoulder at ~255 nm. Surprisingly, the intensity of this feature maximizes at 3 mol equiv of Cu(I) and not at 6 mol equiv as in the atomic absorption analysis of binding stoichiometry. The CD spectrum (Figure 7B) of the synthetic Cu_6NcMT has a positive band at 260 nm and a negative band at 292 nm with a negative shoulder at ~325 nm. Similar to the absorption data, the CD feature at 260 nm increases only up to 3 mol equiv of Cu(I); however, for additional mole equivalents up to 6, there is a decrease in the 260-nm intensity to about 50% that of the 3 mol equiv spectrum (data not shown).

Discussion

In order to lay the groundwork for primary structural modification of metallothionein (MT) and to optimize procedures for preparing peptides with high Cys content, this study has undertaken the solid-phase peptide synthesis of the individual α and β domains from human liver MT-2 and the entire NcMT. During purification we chose to focus on obtaining peptides of high purity and have achieved levels of 90–95% as determined by analytical reversed-phase HPLC, which is capable of separating peptide products with minor differences. For example, the acetylated and unacetylated β domain have retention times differing by 1 min on the analytical C_4 column; other synthetic peptides differing from the native domains only in Cys → Ser substitutions have been shown[21] to be resolvable (retention time differences of >1 min) with a C_{18} column. Product yield was a secondary concern, and unoptimized yields were in the 30–50-mg range. The amino acid content of the synthetic peptides (Table I) indicates that the correct residue composition has been achieved. While automated

(21) Dillon, K. G.; Elgren, T. E.; Ciardelli, T. L.; Wilcox, D. E. To be published.

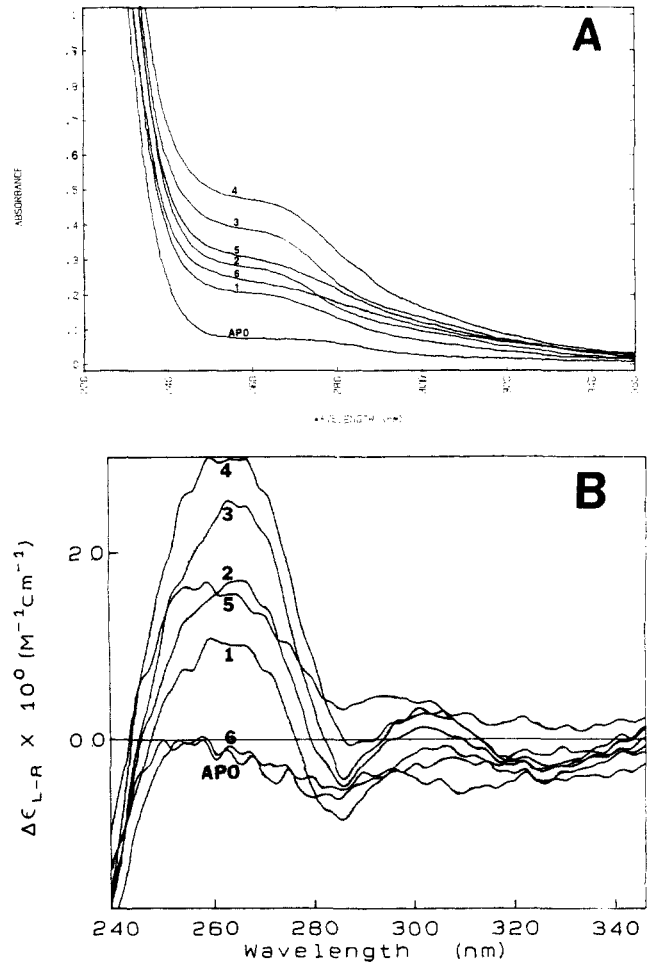

Figure 5. UV absorption (A) and CD (B) spectra of the synthetic α domain in the absence (apo) and presence of increasing mole equivalence of Cu(I).

peptide synthesizers have a high degree of reliability, we have checked the synthetic NcMT protein with an amino acid sequence analysis that confirmed the correct primary structure of this polypeptide. However, to demonstrate that all three synthetic peptides have the same chemical properties as the naturally occurring material, we have examined their metal ion binding with several techniques for comparison to analogous data on native NcMT and the proteolytically derived domains from rat and rabbit liver MT-2; these domains have sequences[1b] nearly identical with that of the human liver MT-2 domains.

β Domain. Cd(II) and Ag(I) binding by the synthetic β domain were monitored by atomic absorption and showed (Figure 1A) a smooth increase in the mole equivalence of metal ion bound to the protein until ratios of ~2.5 and ~5 were reached, respectively. For comparison to the Cd(II) data, (1) Cd(II) binding by displacement of Zn(II) from the Zn-saturated rat liver β domain showed[9] a similar smooth increase, reaching a maximum at 3 mol equiv, (2) addition of 4 mol equiv of Cd(II) to the apo (metal-free) rat liver β domain resulted[9] in recovery of 2.6 mol equiv of Cd(II) bound to the β domain, and (3) proteolytic protection of the rat liver β domain by Cd(II) maximized at 3 mol equiv.[4] Ag(I) binding to the rat liver β domain has been studied[9] by Zn(II) displacement from the Zn-saturated β domain and by Ag(I) protection of the β domain during proteolytic digestion; in the former experiment, a smooth increase in Ag(I) bound to the β domain was observed up to 6 mol equiv of Ag(I), and in the latter experiment, addition of 5–7 mol equiv of Ag(I) to apo-MT prior to subtilisin treatment resulted in 30–40% recovery of the β domain with an average of 5.5 mol equiv of Ag(I) bound. Thus, our synthetic human liver β domain (residues 1–29) binds both Cd(II) and Ag(I) in stoichiometries similar to the rat liver β domain (residues 1–31).

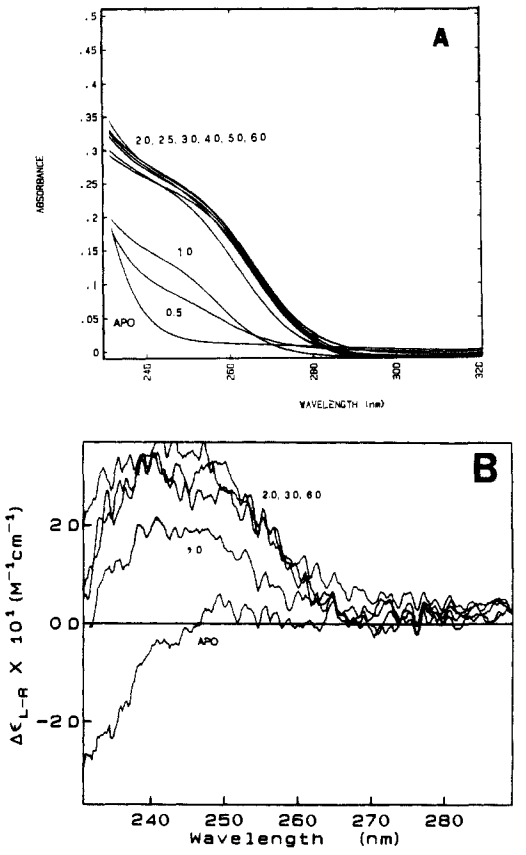

Figure 6. UV absorption (A) and CD (B) spectra of the synthetic NcMT in the absence (apo) and presence of increasing mole equivalence of Cd(II).

Spectroscopic studies of metal ion binding have also been used to characterize the synthetic β domain. Upon Cd(II) addition, new UV absorption intensity is observed with an absorption maximum at 247 nm in the difference spectrum (Figure 2A). This broad feature is indistinguishable from the ~250-nm shoulder observed upon Cd(II) binding to MT from several species[1,22] and the previously synthesized[14b] β domain of human liver MT-2. CD spectra of Cd(II) titrations of both the acetylated and unacetylated synthetic β domain show new features at 250 and 275 nm, which increase in intensity up to 2.5 mol equiv. For comparison, CD has been used to monitor Cd(II) binding to the calf liver β domain,[12b] and there are qualitative similarities in the shape (positive features at ~250 and ~275 nm) and intensities (maximum $\Delta\epsilon > 6\ M^{-1}\ cm^{-1}$) of the calf liver domain CD spectra and that of our synthetic human liver domain. Further, analogous to our synthetic β domain data (Figure 2), >2 mol equiv of Cd(II) led to a decrease in the 250-nm CD intensity of the calf liver β domain; this type of behavior is suggested[12b] to result from Cd(II) cluster formation, exciton coupling of the Cys $RS^- \rightarrow$ Cd(II) CT transitions, and splitting of the CD intensity. Finally, addition of Ag(I) to the synthetic β domain results in a new absorption at 232 nm with a shoulder at ~250 nm. These features, assigned as Cys $RS^- \rightarrow$ Ag(I) CT transitions, appear to be somewhat higher in energy than those reported[23] for the mixed AgZnMT from rat liver.

α Domain. Atomic absorption analysis of Cd(II) and Cu(I) binding to the synthetic α domain (Figure 1B) shows increasing stoichiometries up to 4 mol equiv for Cd(II) and a somewhat higher value of ~6 mol equiv for Cu(I). These data for Cd(II) are consistent with the observation that (1) addition of up to 4 mol equiv of Cd(II) to apo rat liver MT provided[24] increasing yield of the α domain upon subtilisin proteolysis, (2) ≥4 mol equiv of Cd(II) provided[9] maximal resistance of the isolated rat liver α domain to proteolysis, (3) Cd(II) displacement of Zn(II) from the Zn-saturated α domain of rat or rabbit liver MT showed[9] a maximal stoichiometry of 4 mol equiv of Cd(II) bound to the domain, and (4) addition of 4.5 mol equiv of Cd(II) to the apo α domain from rat liver MT resulted in recovery[9] of the domain containing 3.8 ± 0.5 mol equiv of Cd(II). The data for Cu(I) binding to the synthetic α domain are consistent with the observation that (1) addition of up to 5–6 mol equiv of Cu(I) to the apo α domain from rat liver provided[5,9] increasing stabilization of the protein to subtilisin proteolysis, (2) Cu(I) displacement of Zn(II) from the Zn-saturated α domain from rat and rabbit liver led[9] to an increasing amount of Cu(I) bound to the protein up to the addition of 6 mol equiv of Cu(I), and (3) addition of 7 mol equiv of Cu(I) to the apo α domain from rat liver resulted[9] in 6.5 mol equiv of Cu(I) bound to the recovered peptide. However, it was noted[9] that the air sensitivity of Cu(I) resulted in less reproduceable results than found with Ag(I); this likely explains some of the uncertainty in the Cu(I) saturation value (Figure 1B) for the synthetic peptide. Thus, the metal ion binding stoichiometry of our synthetic α domain from human liver MT-2 is consistent with that determined for the proteolytically derived α domain from rat and rabbit liver.

We have used both UV absorption (Figure 3A) and CD (Figure 3B) to monitor Cd(II) titrations of the synthetic α domain. A new shoulder at ~250 nm in the absorption spectrum and new CD features at 238 (−) and 261 (+) nm are observed to increase to a maximal intensity upon addition of ≥4 mol equiv of Cd(II). This electronic data support the Cd(II) stoichiometry determined by atomic absorption analysis. Cd(II) binding to the proteolytically derived rat liver α domain resulted[12a] in an absorption shoulder at ~250 nm and CD features at 239 (−) and 260 (+) nm. While this is entirely analogous to our data on the synthetic α domain, a CD-monitored Cd(II) titration of the proteolytically obtained domain showed[12b] increasing 239- and 260-nm intensity up to 6 mol equiv and then a subsequent decrease in intensity. Our data in Figure 3, however, were for samples that had been treated with Chelex 100 resin to remove loosely bound metal ions and reflect the spectral features of only tightly bound Cd(II); results[12] for the proteolytically derived α domain may show spectral contributions of weakly bound Cd(II) ions beyond the tightly bound 4 mol equiv not removed by cation-exchange resin.

We also have obtained proton-decoupled ^{113}Cd NMR data (Figure 4) for a ^{113}Cd(II)-reconstituted form of our synthetic α domain. The relatively sharp peaks observed at 669, 630, and 627 ppm (50 mM Tris (pH 7.1), 0.5 M NaCl) are in excellent agreement with the resonances associated with Cd(1), Cd(5), and Cd(6) in Cd_7MT-2 from human liver (669.6, 630.8, and 625.4 ppm; 10 mM Tris (pH 9.1), 0.1 M NaCl)[25] and in the proteolytically derived Cd_4 α domain from rat liver (663, 625, and 620 ppm; 0.1 M phosphate (pH 7.9)):[6] note that a 5–7 ppm upfield offset appears[6] to be associated with different pH and ionic strength conditions of the proteolytically derived domain sample. The chemical shift of the fourth Cd(II) in the α domain is reported at 611.9 ppm in the whole human MT[25] and at 612 ppm in the isolated rat liver α domain;[6] thus, accounting for the spectral offset associated with sample conditions, this ^{113}Cd resonance shifts downfield ~6 ppm upon proteolytic isolation of the α domain. This feature is associated with Cd(7) located near the Lys-(30)-Lys(31) linkage to the β domain and is thought to be in a somewhat different environment upon separation of the α domain. This resonance in the whole protein is also most susceptible to shifting upon changes in ionic strength.[26] For the synthetic $^{113}Cd_4$ α domain, a broad feature is observed at 605 ppm that has comparable intensity to the other three resonances and may be associated with this fourth Cd. However, resonances in this region have been associated[27] with dimeric forms of MT that appear upon

(22) Kagi, J. H. R.; Vallee, B. L. *J. Biol. Chem.* **1961**, *236*, 2436–2442.
(23) Winge, D. R.; Premakumar, R.; Rajagopalan, K. V. *Arch. Biochem. Biophys.* **1975**, *170*, 242–252.
(24) Nielson, K. B.; Winge, D. R. *J. Biol. Chem.* **1983**, *258*, 13063–13069.
(25) Boulanger, Y.; Armitage, I. M. *J. Inorg. Biochem.* **1982**, *17*, 147–153.
(26) Vasak, M.; Hawkes, G. E.; Nichols, J. K.; Sadler, P. J. *Biochemistry* **1985**, *24*, 740–747.

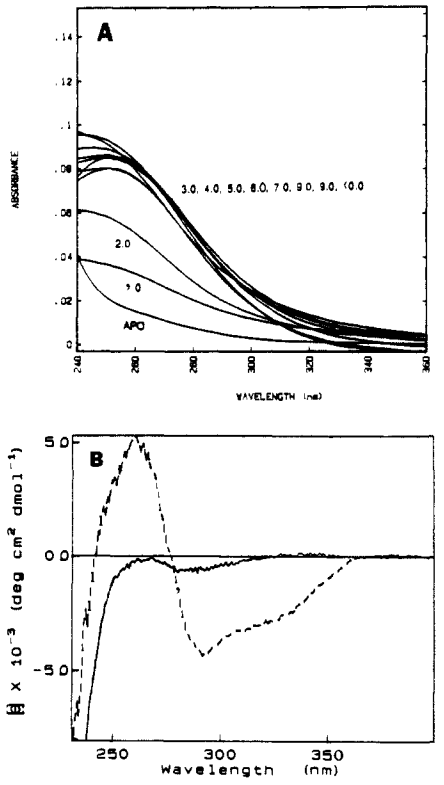

Figure 7. (a) UV absorption spectra of the synthetic NcMT in the absence (apo) and presence of increasing mole equivalence of Cu(I); (B) UV CD spectra of the synthetic NcMT in the absence (—) and presence (- - -) of 6 mole equivalence of Cu(I).

metal ion reconstitution; a weak shoulder at 673 ppm in our NMR spectrum has also been correlated with MT dimers. The other weak feature in Figure 4 is found at 619 ppm and, accounting for the 5–7 ppm offset, occurs at a similar frequency as Cd(7) in the proteolytically derived α domain. Thus, the best interpretation of the ^{113}Cd NMR data for the synthetic Cd_4 α domain is that upon metal ion reconstitution three of the Cd(II)'s are bound in environments identical with that of the native domain; the environment of the fourth Cd(II), however, is more susceptible to perturbation by the absence of the adjacent β domain, environmental factors (ionic strength, pH, etc.), and the formation of MT (and possibly α domain) dimers that have yet to be structurally characterized.

Upon binding of Cu(I) to the synthetic α domain, a new spectral feature at 260–265 nm is observed (Figure 5) in both the absorption and CD spectra. These bands and weaker CD features at wavelengths >280 nm increase in intensity up to 4 mol equiv of Cu(I), paralleling the atomic absorption data on Cu binding. Cu_{12}MT exhibits similar spectral features; however, the specific absorption and CD contributions from Cu(I) binding to the α domain can be estimated from data[28] on Cu(I) displacement of Zn(II) from Zn-saturated MT, since electronic features associated with Zn(II) binding to MT appear at higher energy than those found with Cu(I). Cu(I) preferentially displaces Zn(II) bound to the β domain until 6 mol equiv of Cu(I) is bound; Cu(I) in excess of 6 mol equiv then binds to the α domain displacing the remaining Zn(II). Data for such a titration show[28] increased absorption and positive CD intensity at ~260 nm upon addition of 6–12 mol equiv of Cu(I). Cu(I) displacement of the Cd(II) and Zn(II) from the proteolytically obtained Cd,Zn α domain from rat liver MT has also been studied.[12a] However, overlap of the Cd(II) and Cu(I) spectral features prevents a comparison to our Cu(I) titration data for the apo synthetic α domain. The decrease in both absorption and CD intensity (Figure 5) upon addition of 5 and 6 mol equiv of Cu(I) was unexpected. Cu(I) binding to apo-NcMT, though, also shows decreased CD intensity upon Cu(I) saturation. The strong negative CD data found upon addition of >6 mol equiv of Cu(I) to the synthetic α domain, however, suggest that the decreased CD intensity found with 5 and 6 mol equiv of Cu(I) may be a result of overlapping spectral contributions from the 1–4 mol equiv form and an excess (>6 mol equiv) Cu(I) form of the peptide. The structural and electronic properties of various Cu(I) forms of the α domain are the subject of continuing investigation.

NcMT. Both Cd(II) and Cu(I) binding to the synthetic NcMT have been studied, and atomic absorption analysis shows (Figure 1C) that 2 and 6 mol equiv of these metal ions, respectively, are bound to the 25-residue peptide. NcMT has been reported[29] to bind three Cd(II)'s. However, this stoichiometry was determined on apo samples reconstituted with excess metal ion that may lead[27] to dimerized forms of the protein and different metal-to-peptide ratios. The Cd(II) titration procedure used here should minimize this potential complication, lending confidence to the observed Cd stoichiometry of 2 mol equiv. This discrepancy is not likely due to weakly bound Cd(II) since reconstitution of the native[29] and synthetic protein was accompanied by treatment with Chelex 100. The Cu(I) stoichiometry of 6 mol equiv is identical with that found[2] in the native CuNcMT.

Cd(II) binding to the synthetic NcMT gives rise (Figure 6) to an absorption shoulder at ~250 nm and a positive CD peak at 245 nm; these features are identical with those seen[29] for the Cd(II)-reconstituted native NcMT. Both features increase in intensity until 2 mol equiv of Cd(II) has been added, thus supporting the stoichiometry of the synthetic peptide as determined by AAS. Further, an identical saturation at 2 mol equiv was observed[29] when the absorbance was monitored at 240 nm during a Cd(II) titration of native apo NcMT.

Cu(I) binding to the synthetic NcMT is characterized (Figure 7) by an absorption shoulder at ~255 nm and CD features at 260 (+) and 292 (–) nm; these are very similar to those reported[30] for native CuNcMT. Monitoring Cu(I) addition to the synthetic NcMT, however, shows that the absorbance intensity increases up to 3 mol equiv but shows no additional intensity associated with binding of the next three Cu(I) ions. By comparison, the positive CD intensity at 270 nm increases up to 3 mol equiv but then decreases by about 50% during addition of the remaining three Cu(I)'s (data not shown). While there are no comparable titration data for Cu(I) binding to the native apo-NcMT, this would suggest that the first three ions bind to all seven Cys, resulting in the maximum Cys $RS^- \rightarrow$ Cu(I) CT intensity (dipole moment) in the absorption spectrum and that binding of the remaining Cu(I)'s leads to a different structure, altering the chirality of the metal–protein complex and diminishing the circular dichroism associated with the Cys $RS^- \rightarrow$ Cu(I) CT transition(s). This interesting observation is under further investigation.

Summary

We have now shown that solid-phase peptide synthesis can be used to prepare the individual domains of MT and the whole NcMT and that these synthetic peptides exhibit metal ion binding properties identical with those of the proteolytically derived domains and natural NcMT. We are now exploiting this technique for systematic primary sequence modification of the MT domains and NcMT to further elucidate and quantify the metal ion binding properties of these polythiolate proteins. In addition to being the first report of a successful solid-phase synthesis of this class of peptides, this study demonstrates that careful use of recently developed procedures in solid-phase peptide chemistry now allows the preparation of Cys-rich peptides without irreversible oxidative complications and establishes a suitable protocol for solid-phase preparation of peptides with high Cys content.

(27) Otvos, J. D.; Engeseth, H. R.; Hehrli, S. *Biochemistry* **1985**, *24*, 6735–6740.
(28) Stillman, M. J.; Law, A. Y. C.; Cai, W.; Zelazowski, A. J. Reference 1b, pp 203–211.
(29) Beltramini, M.; Lerch, K.; Vasak, M. *Biochemistry* **1984**, *23*, 3422–3427.
(30) Beltramini, M.; Lerch, K. *Biochemistry* **1983**, *22*, 2043–2048.

Acknowledgment. We thank Paul R. Shafer and David J. Robinson for assistance with the NMR measurements; the NMR spectrometer was purchased in part with funds from the National Science Foundation. We thank Charles C. McCormick for helpful discussions and assistance with the amino acid sequence analysis. F.J.K. and M.F.R. thank the Richter Memorial Trust for Research Grant Awards that supported this research, which was also aided by Grant IN-157B from the American Cancer Society.

Registry No. MT-2 (α-domain), 124650-77-7; MT-2 (β-domain), 124620-43-5; NcMT, 73665-13-1; $CdCl_2$, 10108-64-2; Ag(I), 14701-21-4; $Cu(CH_3CN)_2Cl$, 124685-75-2; ^{113}Cd, 14336-66-4.

Oxidative Addition of Carbon–Oxygen and Carbon–Nitrogen Double Bonds to $WCl_2(PMePh_2)_4$. Synthesis of Tungsten Metallaoxirane and Tungsten Oxo- and Imido-Alkylidene Complexes

Jeffrey C. Bryan and James M. Mayer*,[1]

Contribution from the Department of Chemistry, University of Washington, Seattle, Washington 98195. *Received June 12, 1989*

Abstract: WCl_2L_4 (**1**, L = $PMePh_2$) reacts rapidly with a variety of ketones and aldehydes to form bis(η^2-ketone) or bis(η^2-aldehyde) complexes $WCl_2(\eta^2\text{-}O{=}CRR')_2L_2$ (**2**, **3**). When the ketone is part of a five-membered ring (cyclopentanone, 2-indanone, etc.), **2** rearranges with loss of ketone to give tungsten(VI) oxo–alkylidene products, $W(O)(CRR')Cl_2L_2$ (**4**) in high yield. The net reaction is insertion of the tungsten center into the ketone carbon–oxygen double bond, a four-electron oxidative addition. Insertion into the carbon–nitrogen double bond of *N*-cyclopentyl-*p*-toluidine yields the analogous imido–alkylidene complex $W(N\text{-}Tol)[C(CH_2)_4]Cl_2L_2$. With other ketones, an oxo–alkylidene product is observed only in the reaction of **1** with 1 equiv of ketone and is not seen on decomposition of **2**. This is due to further reaction of the alkylidene complex with free ketone. Aromatic ketones such as benzophenone react with **1** apparently by a radical pathway to give $W(O)Cl_2L_3$ and the olefin derived from two ketones ($Ph_2C{=}CPh_2$), without formation of an observable bis(ketone) intermediate. The two-electron oxidative addition of heterocumulenes is also observed: for example CO_2 is cleaved to form the oxo–carbonyl complex $W(O)(CO)Cl_2L_2$. These are remarkable reactions because of the strength of the carbon–oxygen double bonds being cleaved under very mild conditions. A substantial driving force for the reactions is the formation of a tungsten–oxygen multiple bond, which is estimated to be >138 kcal/mol. The mechanism of double-bond cleavage is proposed to involve an η^2-ketone or cumulene adduct. Based on the spectroscopic data for compounds **2** and **3** and the X-ray crystal structure of the bis(acetone) adduct **2g**, the η^2-ketone intermediates are best described as three-membered rings (metallaoxiranes). The oxo–alkylidene products are apparently formed upon opening of this ring. The preference for these two- or four-electron double-bond oxidative addition reactions versus one-electron (radical) chemistry is discussed.

Oxidative addition reactions are traditionally defined in terms of the scission of a single bond into two monovalent fragments. The oxidative additions of H_2 and MeI to Vaska's complex, $IrCl(CO)(PPh_3)_2$, are typical examples of this fundamental and well-studied transition-metal reaction.[2] In these reactions there is a formal two-electron transfer from the metal to the substrate: two nonbonding electrons on the d^8 iridium center become involved in metal–ligand bonding in the d^6 product.

This paper describes a new type of oxidative addition reaction in which a double bond is cleaved to form two divalent ligands.[3] Ketones and imines oxidatively add to the tungsten(II) complex $WCl_2(PMePh_2)_4$ (**1**),[4] forming tungsten oxo- and imido–alkylidene complexes (eq 1[5]). These are *four*-electron oxidative addition reactions, as four nonbonding electrons in **1** are converted to tungsten–ligand bonding electrons in the tungsten(VI) products.

Scheme I

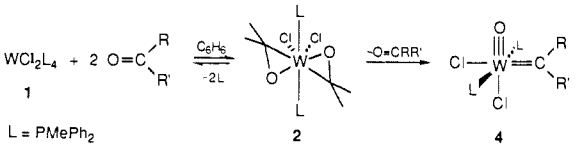

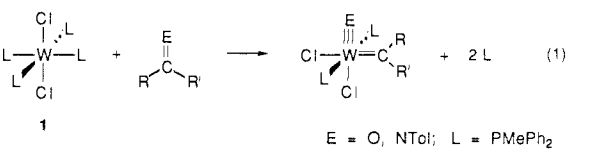

E = O, NTol; L = $PMePh_2$ (1)

The oxidative addition of heterocumulenes such as carbon dioxide and isocyanates (eq 2) also involves simple insertion of

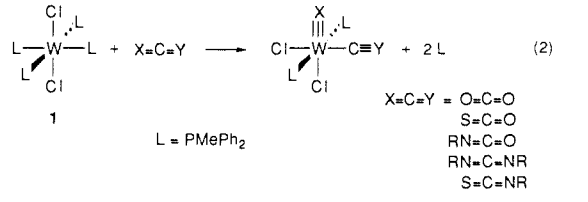

X=C=Y = O=C=O, S=C=O, RN=C=O, RN=C=NR, S=C=NR (2)

(1) Presidential Young Investigator, 1988–1993; Sloan Foundation Fellow, 1989–1991.

(2) (a) Collman, J. P.; Hegedus, L. S.; Norton, J. R.; Finke, R. G. *Principles and Applications of Organotransition Metal Chemistry*; University Science Books: Mill Valley, CA, 1987; Chapter 5. (b) Lukehart, C. M. *Fundamental Transition Metal Organometallic Chemistry*; Brooks/Cole: Monterey, CA, 1985; Chapter 10.

(3) Portions of this work have been published: Bryan, J. C.; Mayer, J. M. *J. Am. Chem. Soc.* **1987**, *109*, 7213-7214.

(4) (a) Sharp, P. R. *Organometallics* **1984**, *3*, 1217-1223. (b) Sharp, P. R.; Bryan, J. C.; Mayer, J. M. *Inorg. Synth.*, in press.

(5) Tungsten–oxygen and tungsten–nitrogen multiple bonds are written as triple bonds because that is the best description in typical coordination environments. See Chapter 2 of ref 5a. (a) Nugent, W. A.; Mayer, J. M. *Metal–Ligand Multiple Bonds*; Wiley-Interscience, New York, 1988.

0002-7863/90/1512-2298$02.50/0